Colloids and Surfaces B: Biointerfaces 113 (2014) 85–91

Contents lists available at ScienceDirect

Colloids and Surfaces B: Biointerfaces

journal homepage: www.elsevier.com/locate/colsurfb

Detection of real sample DNA at a cadmium sulfide – chitosan/gelatin modified electrode

Ying Li [a], Wan-Chun Chen [a], Shen-Ming Chen [a,*], Bih-Show Lou [b,**], M. Ajmal Ali [c], Fahad M.A. Al-Hemaid [c]

[a] Electroanalysis and Bioelectrochemistry Lab, Department of Chemical Engineering and Biotechnology, National Taipei University of Technology, No. 1, Section 3, Chung-Hsiao East Road, Taipei 106, Taiwan, ROC
[b] Chemistry Division, Center for General Education, Chang Gung University, Tao-Yuan, Taiwan
[c] Department of Botany and Microbiology, College of Science, King Saud University, Riyadh 11451, Saudi Arabia

ARTICLE INFO

Article history:
Received 26 March 2013
Received in revised form 18 August 2013
Accepted 20 August 2013
Available online xxx

Keywords:
Cadmium sulfide (CdS)
Chitosan (*Chi*)
Gelatin (*Gel*)
Guanine (G)
Adenine (A)
Modified electrodes

ABSTRACT

Cadmium sulfide (CdS) was combined with chitosan (*Chi*) and gelatin (*Gel*) to prepare a CdS-*Chi*/*Gel* modified electrode. *Chi* exhibits a large positive charge density and was to provide a uniform of CdS surface. *Gel* exhibits high mechanical strength and low toxicity toward mammalian cells, and is non-antigenic biopolymer. CdS-*Chi* exhibits a lower contact angle than that of bare CdS, indicating that the hydrophilicity of the sample surface had increased. Electrochemical impedance spectroscopy (EIS) was used to determine diffusion coefficients and to characterize the electron transfer kinetics during the redox reactions. The surface morphologies of CdS-*Chi* and *Gel* were characterized using scanning electron microscopy (SEM) and atomic force microscopy (AFM). Differential pulse voltammetry (DPV) was used to detect the analytes. DPV not only increased the linear range of the electrocatalytic current, but also lowered the overpotential for oxidation interference in the measurements. The CdS electrode exhibited a enhanced electrocatalytic activity toward the analytes evaluated in this study. The presence of *Gel* enhanced the loading and stability of the electrode. The fabricated electrode was successfully used for the simultaneous electrochemical oxidation of guanine (G) and adenine (A).

1. Introduction

Deoxyribonucleic acid (DNA) is a well-known natural macromolecule that consists of four bases, guanine (G), adenine (A), thymine (T) and cytosine (C), and is an important biological molecule that plays a critical role in the storage of genetic information and protein biosynthesis [1–4]. Several analytical methods have been developed to detect DNA bases [5,6]. In recent years, a variety of new and intriguing techniques have been developed to overcome the above limitations, such as fluorescence resonance energy transfer [7], surface plasmon resonance (SPR) [8], optofluidic ring resonators [9], colorimetric assays [10], bipartite split-luciferase sensors [11], electrochemiluminescence [12,13], surface enhanced Raman spectroscopy [14], microchip capillary electrophoresis [15–17], flow injection chemiluminescence [18,19], ionpairing liquid chromatography [20,21], laser-induced fluorescence detection [22,23], and micellar electrokinetic chromatography [24,25].

Importantly, electrochemical DNA sensors possess enormous potential for the, simple, low-cost and on-site detection of contaminants for clinical monitoring [26,27]. Electrochemical techniques have the promising ability to evaluate the DNA methylation state in a rapid, convenient and accurate way [28–32]. The electrocatalytic oxidation of purine bases has been extensively investigated in the literature [33–36]. In general, DNA biosensors have emerged as a promising alternative for microbial detection due to the specificity of hybridization between probe DNA and the complementary target sequence [37]. However, the occurrence of non-specific adsorption during the hybridization process necessitates the development of a more sensitive and specific DNA biosensor. Electrochemical detection of pyrimidine bases has rarely been studied. Traditional solid electrodes often suffer from fouling effects due to the accumulation of oxidized products on the electrode surface, resulting in poor sensitivity and reproducibility [38,39]. High oxidation potentials cause large background currents in blank solutions, which severely mask peak currents and adversely affect the detection sensitivity [40,41]. The electrochemical oxidation of pyrimidine bases is irreversible. It is difficult to obtain accurate oxidation signals from pyrimidine bases due to their extremely positive oxidation

* Corresponding author. Tel.: +886 2270 17147; fax: +886 2270 25238.
** Corresponding author. Tel.: +886 3211 8800x5018; fax: +886 3211 8700.
E-mail addresses: smchen78@ms15.hinet.net (S.-M. Chen), blou@mail.cgu.edu.tw (B.-S. Lou).

0927-7765/$ – see front matter © 2013 Elsevier B.V. All rights reserved.
http://dx.doi.org/10.1016/j.colsurfb.2013.08.028

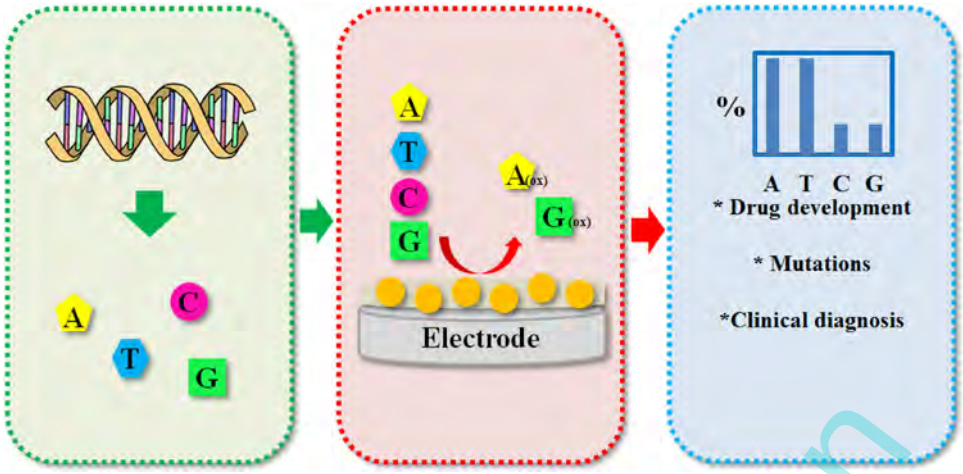

Scheme 1. Electrochemical oxidation of guanine (G) and adenine (A) using the CdS-*Chi*/*Gel*-modified electrode.

potentials and slow electron transfer kinetics [42,43]. To overcome these limitations, modified nanomaterial-based electrodes with a wide potential window, high electrocatalytic activity and excellent antifouling properties are necessary.

Nanomaterials have emerged a promising class of functional materials for their versatile roles, in high throughput optoelectronic devices as well as in the ultrasensitive, direct electrical detection of biological and chemical species [44,45]. They exhibit unique optical, electrochemical and catalytic properties, and their small size allows the miniaturization of the sensor device. In particular, metal and semiconductor nanoparticles have attracted considerable attention due to their controlled porosities, high loading volumes, and large surface areas [46–49]. Compared with their thin film counterparts, nanoparticles possess a larger surface-to-volume ratio, uni-directional conduction channels, and diameters on the same size scale as the molecules being detected. These properties have generated considerable interest in the use of nanoparticles as bioelectrochemical transducers. Remarkably, the conductance of nanoparticles is extremely sensitive to small surface perturbations. Gold, silver or platinum nanoparticles, as well as semiconducting biosensors [50–52] such as CdS, ZnS or PbS, exhibit excellent biocompatibility and are easily conjugated to biological materials [53]. It is evident that, the large surface areas of conductive nanomaterials can increase molecule loading and facilitate the reaction kinetics, thus improving the biocatalytic processes of the biosensor. In addition, efforts have also been made to improve the activity and stability of immobilized biomolecules using nanostructures. For example, TiO_2 nanoparticles and Au nanoparticle modified electrodes have been also used for the electrocatalytic detection of guanine and adenine [54,55]. Another study presented a label-free fluorescent method for the measurement of PNK activity using double-stranded DNA (dsDNA)-templated copper nanoparticles (CuNPs) as a fluorescent indicator [56]. Recently, various nanobiocatalytic approaches have gained increasing attention due to their successful applications in biomolecule stabilization. In light of these recent advances, we expect that further progress in nanostuctured biocatalysts will play a critical role in overcoming major obstacles in biosensor development.

In this study, we exploited the unique properties of CdS nanoparticles (CdS NPs) for modified electrodes (Scheme 1). Chitosan (*Chi*) and gelatin (*Gel*), as simple and readily available materials, were used to enhance the electrode stability. CdS is an important material in the development of new varieties of biosensors, H_2-production systems and *in vivo* power supplies. To develop a successful electrochemical detection system, high sensitivity, signal amplification and good selectivity are crucial. DNA has been extensively used as a versatile material for in the construction of biosensors due to the simplicity and predictability of its secondary structure.

2. Experimental

2.1. Materials

Cadmium chloride ($CdCl_2$), thioacetamide (TAA, C_2H_5NS), chitosan (*Chi*), gelatin (*Gel*) guanine (G), adenine (A) and DNA (from *salmon testes*) were purchased from Sigma–Aldrich (USA). All other chemicals were of analytical grade and were used without further purification. Phosphate buffered saline (PBS) (pH 7.0, 0.1 M Na_2HPO_4 and 0.1 M NaH_2PO_4) and acetate buffer (pH 5.0) were used as the supporting electrolytes. Aqueous solutions were prepared using double-distilled deionized water and then de-aerated by purging with high purity nitrogen gas for approximately 20 min prior to performing the electrochemical experiments. In addition, a continuous flow of nitrogen over the aqueous solution was maintained during the measurements. Indium tin oxide (ITO) (7 Ω/cm^{-2}) was purchased from Merck Display Technologies (MDT) Ltd. (Taiwan).

2.2. Apparatus

Water contact angles were measured by the micro syringe drop method using the CMA110 system. The contact angles were reported as the averaged value of a minimum of five measurements. Cyclic voltammetry (CV) was performed in using the model CHI-1205B, and differential pulse voltammetry (DPV) was conducted using a CHI-900 and CHI-410 potentiostat. A conventional three-electrode cell assembly consisting of an Ag/AgCl reference electrode and a Pt wire counter electrode were used for the electrochemical measurements. The working electrode was a glassy carbon electrode (GCE; area 0.07 cm^2). The potentials were reported *vs.* the Ag/AgCl reference electrode. The morphologies of the films were examined using scanning electron microscopy (SEM) (Hitachi S-3000H) and atomic force microscopy (AFM) (Being Nano-Instruments CSPM5000). Electrochemical impedance spectroscopy (EIS) measurements were performed using an IM6ex Zahner instrument (Kroanch, Germany). All experiments were performed at room temperature (≈25 °C).

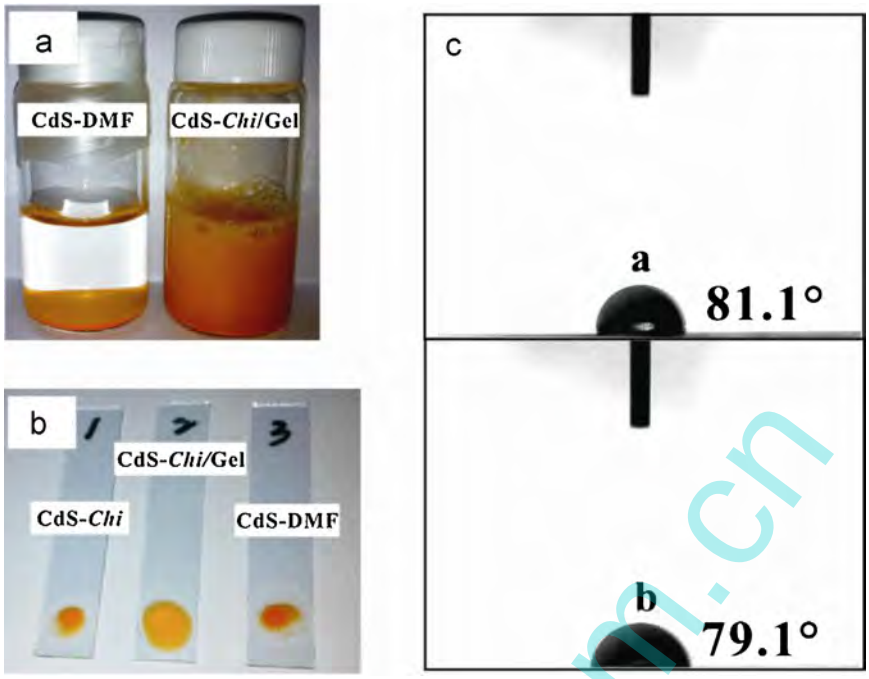

Fig. 1. (A) Individual suspensions in different solvent conditions: CdS-DMF and CdS-*Chi*/*Gel*. (B) Various pastes were dropped onto the ITO surface to form films of CdS-*Chi*, CdS-*Chi*/*Gel* and CdS-DMF. (C) Contact angles were measured at 25 °C by the micro syringe drop method. Values are reported as the average of at least five measurements. The contact angles of (a) untreated (CdS-water) and (b) treated (CdS-*Chi*) samples on ITO were 81.1° and 79.1°, respectively.

2.3. Preparation of CdS-Chi/Gel-modified electrodes

2.3.1. Preparation of CdS NPs

CdS NPs were synthesized according to previous reports, with some modifications. Briefly, 1.78 g of $CdCl_2$ and 2 g of thioacetamide (TAA) were dissolved in 100 mL of deionized water and continuously stirred for 30 min to allow complete dissolution. The synthesis of CdS using TAA as the S^{2-} source is described in Eq. (1). The solution was then transferred to a centrifuge tube and yielded a yellow precipitate, which was harvested by centrifugation. To remove any remaining cations or anions, the precipitate was washed several times using deionized water and ethanol. The suspension was dried in an oven at 70 °C for 24 h. Finally, the products were calcined at 350 °C for 2 h for further characterization.

$$Cd^{2+} + CH_3C(S)NH_2 + H_2O \rightarrow CdS_{(s)} + CH_3C(O)NH_2 + 2H^+ \quad (1)$$

2.3.2. Preparation of Chi, Gel, and DNA solutions

A CdS-*Chi* solution (7 mg/mL) was prepared from 0.035% *Chi* in pH 5.0 acetate buffer and sonicated for 10 min to obtain a homogeneous mixture. A 4% CdS-*Chi*/*Gel* paste was fabricated from the CdS-*Chi* solution using *Gel* powder and heated to 50 °C until full melting was achieved. The double-stranded (dsDNA) sample was treated in pH 13 NaOH buffer solution. This extreme pH condition forced the denaturation of the dsDNA to single-stranded (ssDNA), ensuring that the bases (A, T, C and G) were exposed.

2.3.3. Preparation of modified electrodes

Prior to modification, the glassy carbon electrode (GCE) was polished with 0.05 μm alumina on Buehler felt pads and then ultrasonically cleaned for approximately 1 min in water. Finally, the electrode was washed thoroughly with double-distilled water and dried at room temperature. A 2 μL volume of the CdS-*Chi*/*Gel* paste was dropped onto the polished GCE surface and allowed to evaporate to dryness for the electrochemical experiments. Prior to modification, the ITO surfaces were cleaned and ultrasonicated in an acetone–water mixture for 15 min and then dried. The same volum of CdS-*Chi*/*Gel* paste was dropped onto the ITO for subsequent morphological characterization.

3. Results and discussion

3.1. Physical characterization of the CdS-Chi/Gel paste

To investigate the effect of solvents on the stability of the *Chi*/*Gel* electrode coating, a series of materials was prepared from the mixtures. *Chi* and *Gel*, which are commonly used to disperse nanomaterials, were tested for their ability to disperse the CdS nanoparticles in order to prepare a stable and sensitive modifying layer on the GCE surface. Fig. 1(A) displays the individual suspensions in various solvent conditions. A conventional organic solvent, dimethylformamide (DMF), was used to disperse the CdS. *Chi* is a polysaccharide derived from the deacetylation of chitin. It contains primary amino groups with a pK_a value of approximately 6.3, as well as a highly positive charge density. Due to its positive charge, *Chi* can effectively homogenize mixtures. Compared with CdS-DMF, the CdS-*Chi*/*Gel* preparation exhibited better dispersion. Fig. 1(B) depicts modified electrodes prepared from CdS-*Chi*, CdS-*Chi*/*Gel* and CdS-DMF. The various dispersions were dropped in 4 μL aliquots onto ITO surfaces. CdS-*Chi* and CdS-DMF contained aggregats and exhibited rough surfaces on the electrode. In contrast, the CdS-*Chi*/*Gel*-modified electrode was well-dispersed and smooth. Fig. 1(C) displays the contact angle reports, with the angle values representing the average of at least five measurements. The contact angles were measured at 25 °C by the micro syringe drop method. The contact angle, which is a measure of surface wettability, was used to determine the hydrophobicity or hydrophilicity of the modified surfaces. The (a) untreated (CdS-water) and (b) treated (CdS-*Chi*) samples on the ITO surface exhibited contact angles of 81.1° and 79.1°, respectively. These low contact angles indicate that the samples displayed a hydrophilic surface. *Chi* is a hydrophilic, biodegradable [57], non-antigenic biopolymer that exhibits, high mechanical strength, fast metal complexation, susceptibility to

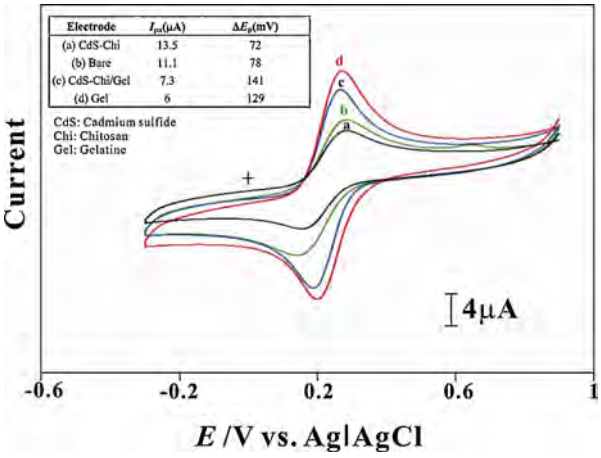

Fig. 2. Cyclic voltammograms (CVs) of (a) CdS-*Chi*-modified, (b) bare, (c) CdS-*Chi*/*Gel*-modified and (d) *Gel*-modified electrodes in pH 7.0 PBS containing 1×10^{-3} M $[Fe(CN)_6]^{3-}$ using a potential range from 0.9 to −0.3 V and a scan rate of 50 mV s^{-1}. The inset displays detailed data for the current values and expanded peak potential separations.

chemical modification [58,59], and a low toxicity toward mammalian cells. Our results revealed that CdS-*Chi*/*Gel* enabled superior stability and dispersion compared with the other evaluated samples; CdS-*Chi*/*Gel* was therefore selected for further optimization in subsequent experiments.

3.2. Electrochemical characterization of the modified electrodes

Each newly-prepared modified electrode was transferred to pH 7.0 PBS containing 1×10^{-3} M $[Fe(CN)_6]^{3-}$ for electrochemical characterization. These optimized pH 7.0 solutions were chosen to improve stability. Cyclic voltammetry was performed at a 50 mV s^{-1} scan rate in the potential range of 0.9 V to −0.3 V. Fig. 2 displays a comparison of the cyclic voltammograms collected from the bare electrode and the CdS-*Chi*, CdS-*Chi*/*Gel* and *Gel*-modified electrodes. The *Gel*-modified electrode exhibited a peak current value and peak potential separation of 6.02 μA and 129 mV, respectively. The bare electrode displayed a peak current value and peak potential separation of 11.15 μA and 78 mV, respectively. The solid state of the gel contributed to the decreased current value and increased peak potential separation. The CdS-*Chi*-modified electrode exhibited a peak current value and peak potential separation of 13.51 μA and 72 mV. The current values and expanded peak potential separations are displayed in the insert. However, by comparing the CVs obtained from the CdS-*Chi*-modified and the bare electrode, it is evident that the CdS significantly improved the electron transfer properties of the sensor. Compared with the other electrodes, the CdS-*Chi*-modified electrode displayed the highest reaction current. Clearly, the CdS exhibited semiconducting properties. The superior properties of the CdS-*Chi*/*Gel* composite compared with CdS-*Chi* composite stemmed from its more stable dispersion on the electrode, as well as the electrostatic interactions between the positively charged *Chi* and negatively charged ferricyanide complexes. The CdS-*Chi*/*Gel*-modified electrode provided numerous advantages compared with the bare and CdS-*Chi* electrodes.

Electrochemical impedance spectra (EIS) can provide information about the impedance changes at the electrode surface for each modification step and be used to monitor the entire electrode modification process. The EIS contained semicircular and linear components. The semicircle parameters corresponded to the electron transfer resistance (R_{ct}) and the double layer capacity (C_{dl}) of the modified electrode. The semicircular component at higher

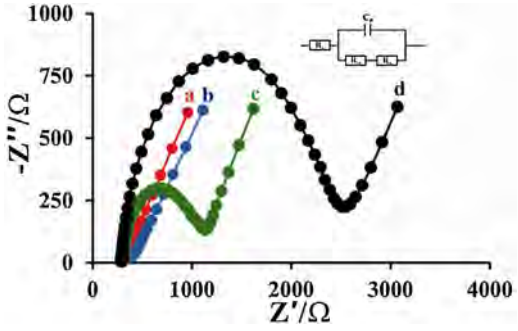

Fig. 3. Electrochemical impedance spectra (EIS) of (a) CdS-*Chi*-modified, (b) Bare, (c) CdS-*Chi*/*Gel*-modified and (d) *Gel*-modified electrodes in pH 7.0 PBS containing 5×10^{-3} M $[Fe(CN)_6]^{-3/-4}$. Amplitude = 5 mV.

frequencies was related to the electron transfer limited process, with the diameter equivalent to R_{ct}. A plot of the real (Z') and imaginary (Z'') components produced a semicircular Nyquist plot. From the shape of the impedance spectrum, the electron-transfer kinetics and diffusion characteristics can be extracted. The linear component at lower frequencies corresponded to the diffusion process. This type of impedance spectrum is characteristic of a surface-modified electrode in which electron transfer is slow and the impedance is controlled by the interfacial electron transfer at high frequencies. Fig. 3 displays the EIS results for the various modified electrodes in the presence pH 7.0 PBS with an equimolar quantity of 5 mM $[Fe(CN)_6]^{3-/4-}$. The Faradaic impedance spectra are presented as Nyquist plots (Z'' *vs.* Z') for the bare electrode and the CdS-*Chi*-, CdS-*Chi*/*Gel*- and *Gel*-modified electrodes. The CdS-*Chi* electrode exhibited a nearly straight line (curve a) with a very small depressed semicircle arc (R_{ct} = 290 (Z'/Ω)), representing the characteristics of a diffusion limited electron-transfer process on the electrode surface. The bare (curve b) and *Gel*-modified (curve d) electrodes exhibited a depressed semicircular arc with an interfacial resistance due to the electrostatic repulsion between the charged surface and the probe molecule $[Fe(CN)_6]^{3-/4-}$. This depressed semicircular arc (R_{ct} = 2550 (Z'/Ω)) revealed that the *Gel*-modified electrode exhibited the highest electron transfer resistance. The R_{ct} of the CdS-*Chi*/*Gel*-modified (curve c) electrodes was 1140 (Z'/Ω). The inset displays the equivalent circuit (Randles model) used to fit the Nyquist diagrams. This circuit contains a distributed element which can only be approximated by an infinite series of simple electrical elements. The error values for the corresponding semicircles ranged from 5% to 7%.

The increase in R_{ct} value occurred due to the embeddeding of the CdS in the *Gel*. These results were in close agreement with those of previous CV studies.

3.3. Morphological characterization of CdS-Chi/Gel-modified electrodes

Prior to modification, the ITO surfaces were cleaned and ultrasonicated in an acetone–water mixture for 15 min and then dried. Subsequently, CdS-*Chi*, *Gel* and CdS-*Chi*/*Gel* films wrer prepared on the ITO and characterized by SEM. From Fig. 4(A–C), significant morphological differences among the films can be observed. The top views of the nano-structures (A) on the ITO electrode surface reveal uniformly deposited and homogeneously dispersed CdS-*Chi* on the electrode. The CdS-*Chi*/*Gel*-modified electrode in (C) displayed a *Gel* coating over the entire CdS surface. A comparison of the CdS-*Chi* (A) and CdS-*Chi*/*Gel* (C) electrodes revealed, that these morphological differences could be attributed to the increase in the deposition of *Gel*, which created plateaus rather than beads and completely covered the CdS. It is evident that the CdS was immersed in the *Gel*.

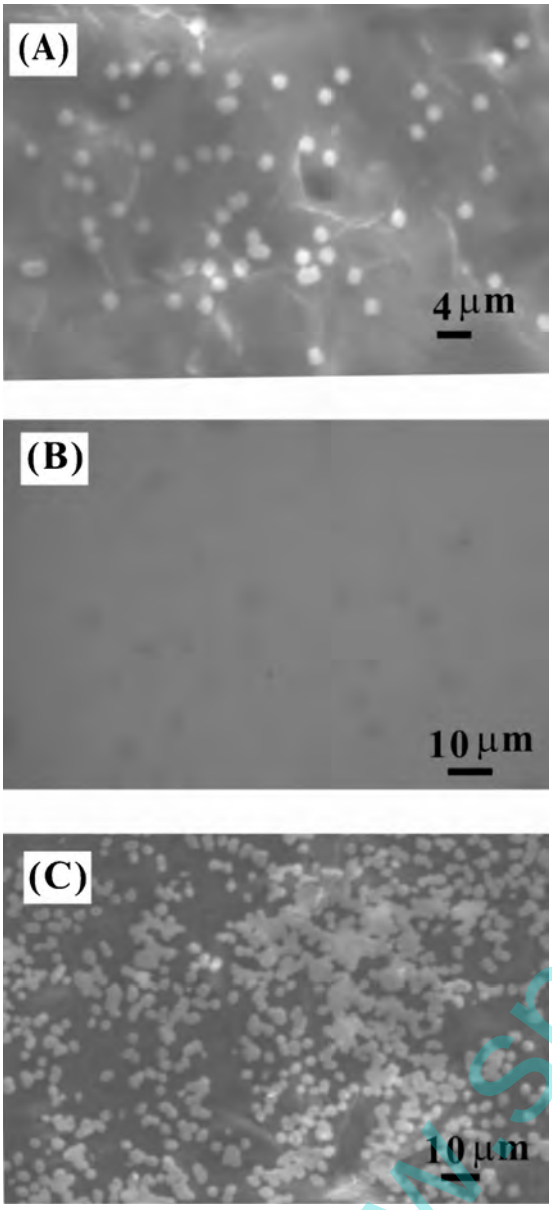

Fig. 4. SEM images of (A) CdS-*Chi*, (B) *Gel* and (C) CdS-*Chi*/*Gel* on an ITO electrode.

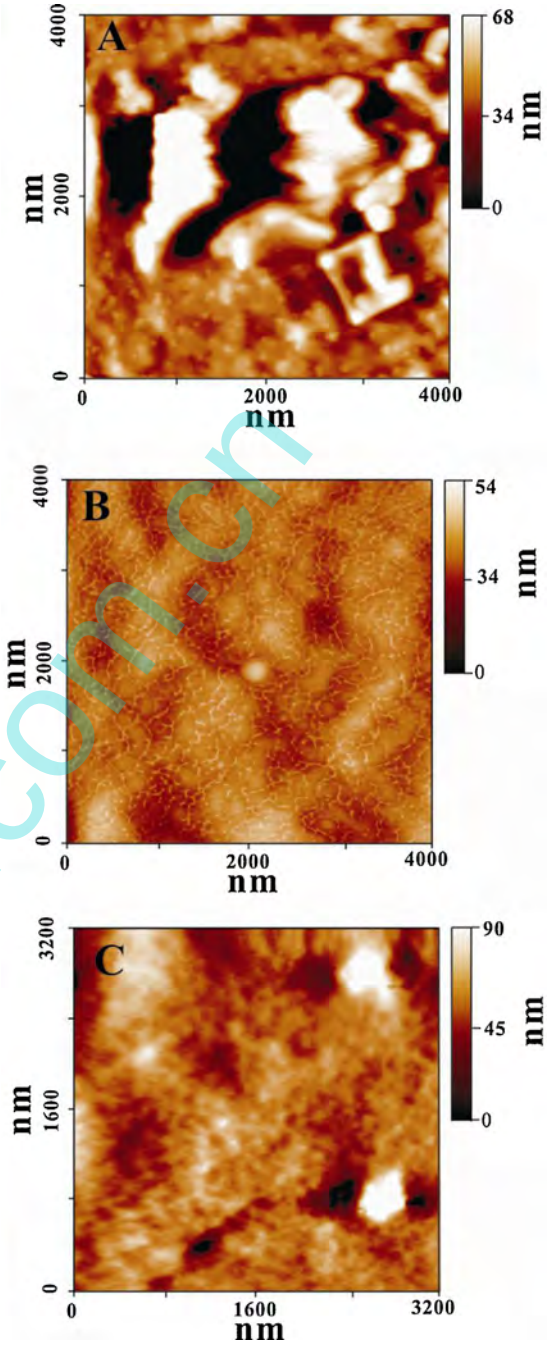

Fig. 5. AFM images of (A) CdS-*Chi*, (B) *Gel* and (C) CdS-*Chi*/*Gel* on an ITO electrode.

The surface morphologies of the electrodes were also examined using AFM. The AFM results provided comprehensive information about the surface morphology of the nanostructures on the ITO surface. The AFM images were collected over 3200 nm × 3200 nm and 4000 nm × 4000 nm surface areas and used to determine the roughness average (sa), an expression of the surface roughness or texture that is typically used to describe a polished or machined metal surface and the arithmetic average value of the departure (peaks and valleys) of the surface profile from the center-line through the sampling length. In addition, the CdS-*Chi*, *Gel* and CdS-*Chi*/*Gel* films on the ITO electrode were characterized using AFM. From Fig. 5(A–C), it is apparent that there are morphological differences among the films. The top views of the nanostructures (A) reveal uniformly deposited and homogeneously dispersed CdS-*Chi* on the electrode. Nanostructures were present with an average height of 33.4 nm. The roughness average (sa) for the CdS-*Chi* was 14.9 nm and the root mean square roughness was 19.2 nm. The grain size analysis revealed an average size of 110 nm. The *Gel*-modified electrode in (B) exhibited a smooth surface with a roughness average (sa) and root mean square roughness of 4.44 nm and 5.62 nm, respectively. The average height and diameter were 26.9 nm and 28.2 nm, respectively. Fig. 5(C) displays an image of the CdS-*Chi*/*Gel*, which exhibited a roughness average (sa) and root mean square roughness of 1.13 nm and 1.54 nm, respectively. The average height and diameter were 4.18 nm and 31.5 nm, respectively. Comparing the CdS-*Chi* (A) and CdS-*Chi*/*Gel* (C) electrodes revealed, a smaller CdS particle size in the presence of *Gel* indicating the role of the *Gel* in the dispersion of the nanoparticles.

3.4. Electrocatalytic reaction of DNA bases at CdS-Chi/Gel modified electrode

The differential pulse voltammetry (DPV) was performed in the presence of different concentrations of guanine and adenine

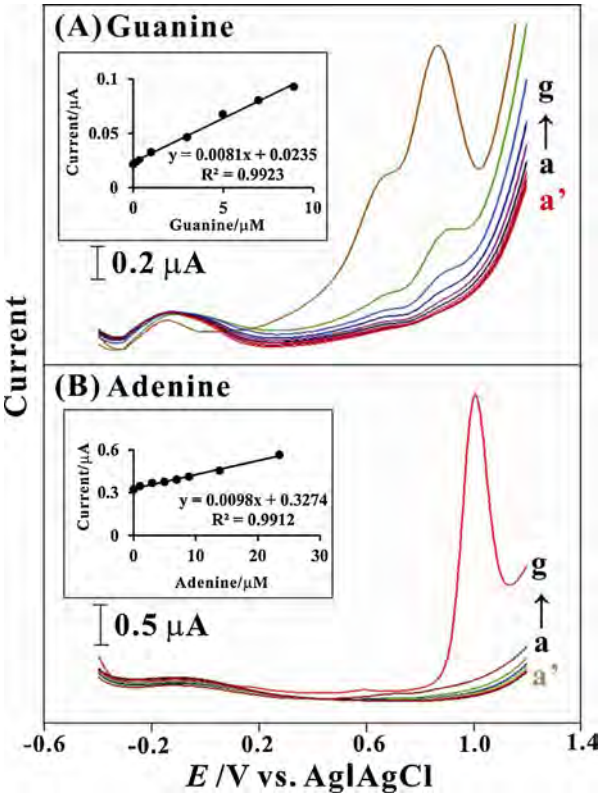

Fig. 6. Differential pulse voltammetry (DPV) measurements of (A) guanine and (B) adenine at a CdS-*Chi*/*Gel*-modified electrode in 0.1 M PBS (pH 7.0) containing varying concentrations (a–g) of the analytes, using a potential range from −0.4 to 1.2 V and a scan rate of 50 mV s^{-1}. The calibration curves for the analytes, are nearly linear for the concentration ranges shown in the inset.

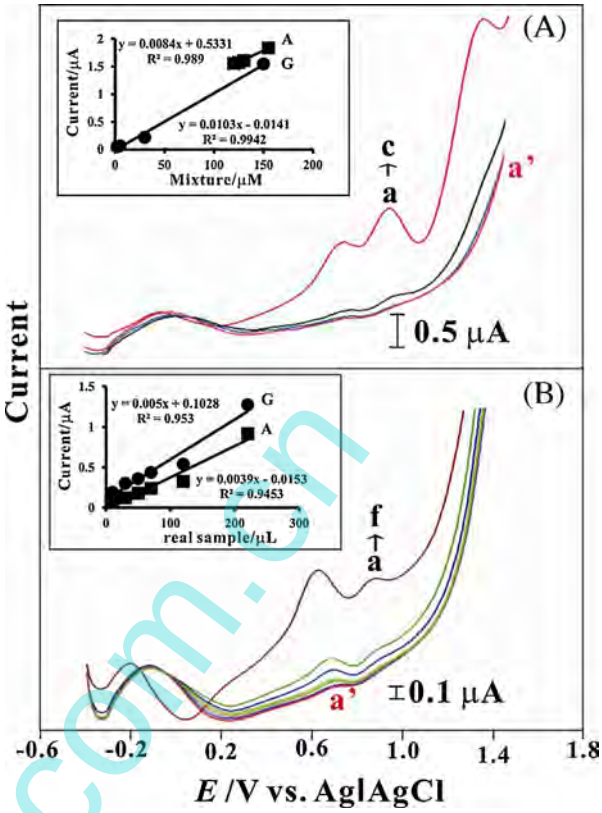

Fig. 7. Differential pulse voltammetry (DPV) measurements of varying concentrations of (A) guanine with adenine and (B) a real DNA sample (from *salmon testes*) at a CdS-*Chi*/*Gel*-modified electrode in 0.1 M PBS (pH 7.0) using a potential range from −0.4 to 1.4 V and a scan rate of 50 mV s^{-1}.

at a CdS-*Chi*/*Gel*-modified electrode in 0.1 M PBS (pH 7.0) over a potential range of −0.4 V to 1.2 V using a scan rate of 50 mV s^{-1}, as depicted in Fig. 6(A and B). The DPV values were recorded at a constant time interval of 2 min, with nitrogen purging performed prior to the start of each experiment. Fig. 6(A) depicts the CdS-*Chi*/*Gel*-modified electrode in the presence of varying concentrations (a–g) of guanine. Interestingly, the peak currents for guanine increased linearly with increasing of guanine concentration. As a result, the calibration curves for guanine, were nearly linear over a wide range of concentrations, as shown in the inset. From this calibration plot, the linear concentration range was 9.9×10^{-7} M to 8.9×10^{-6} M. The inset reveals that the lower and upper bounds for the detection limit of guanine were 9.9×10^{-7} M and 3.28×10^{-5} M, respectively. The electrocatalytic activity exhibited a redox couple at 0.86 V [60]. Fig. 6(B) displays the DPV results for varying concentrations (a–g) of adenine at CdS-*Chi*/Gel-modified electrode. The reaction current for adenine increased linearly with increasing analyte concentration. The calibration curve for adenine, which was nearly linear over a wide range of concentrations, is displayed in the inset. From this calibration plot, a linear response was observed over a concentration range from 9.9×10^{-7} to 2.34×10^{-5} M. The inset reveals that the lower and upper limits of detection for adenine were 9.9×10^{-7} M and 6.89×10^{-5} M, respectively. The electrocatalytic activity exhibited a redox couple at 1.01 V [60]. This peak current response occurred due to the reaction mechanism of guanine and adenine oxidation. Compared with the bare electrode (curve a′) over the same concentration range of guanine and adenine, the CdS-*Chi*/Gel modified electrode exhibited a redox couple and a higher peak current response to the DNA bases. The DPV measurements revealed an increase in the linear concentration range of the electrocatalytic current as well as lower overpotential for oxidation or reduction interference.

3.5. *Electrocatalytic reaction of real DNA sample at CdS-Chi/Gel-modified electrode*

Fig. 7(A) displays the DPV results from the CdS-*Chi*/*Gel*-modified electrode in 0.1 M PBS (pH 7.0) using a potential range of −0.4 V to 1.4 V and a scan rate of 50 mV s^{-1} for the catalytic reduction of guanine and adenine. The catalytic current response is directly proportional to the concentrations of guanine and adenine in the system. The electrocatalytic activity exhibited a redox couple at 0.9 V and 1.2 V. The lower and upper limits of detection for guanine in the presence of adenine were 9.9×10^{-7} M and 1.38×10^{-5} M, respectively. DNA samples (from *salmon testes*) were treated in a pH 13 NaOH buffer solution (1 mg/mL). These extreme pH conditions facilitated the dsDNA denaturation to ssDNA, ensuring that all of the DNA bases were exposed. Using the same conditions, the electrocatalytic activity of the CdS-*Chi*/*Gel*-modified electrode was evaluated in the presence of varying volumes (μL) of the DNA sample. Volumes of the DNA sample varying from 10 μL to 220 μL were added to a 10 mL volume of a blank buffer solution (pH 13). The electrocatalytic activity redox couple shifted to 0.62 V and 0.88 V at pH 13. These results verified that the CdS-*Chi*/*Gel*-modified electrode was capable of producing an electrocatalytic response to real DNA samples. Overall, the CdS-*Chi*/*Gel*-modified electrode was stable and was successfully used for the electrocatalytic oxidation of guanine and adenine. More specifically, the enhanced electrocatalytic activity of the CdS-*Chi*/*Gel*-modified electrode can be attributed to the higher peak current of the CdS. *Gel* was found to promote the stability of the modified electrode (Fig. 8).

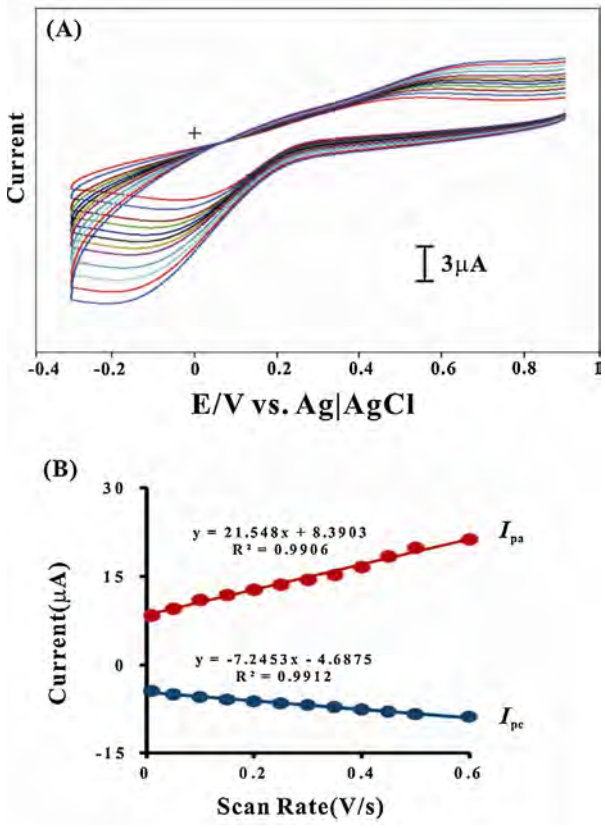

Fig. 8. Different scan rates of the CdS-*Chi*/*Gel*-modified electrode in 0.1 M PBS (pH 7.0) from 10 to 600 mV s^{-1}.

4. Conclusions

The high stability and facile preparation of CdS-*Chi*/*Gel*-modified electrodes make them promising candidates for construction of simple electrochemical biosensors for the detection of DNA bases. Repetitive redox cycling experiments were performed to determine the stability of CdS-*Chi*/*Gel*-modified films in 0.1 M PBS (pH 7.0). This investigation revealed that after 100 continuous scan cycles with a scan rate of 0.1 V s^{-1}, the peak heights of the cyclic voltammograms decreased less than 5%. The CdS-*Chi*/*Gel*-modified film maintained its initial activity for more than three weeks when stored in 0.1 M PBS (pH 7.0). A decrease of 8% was observed in the current response of the electrode after 20 days. We demonstrated the successful application of the CdS-*Chi*/*Gel*-modified electrode to the measurement of guanine (G) and adenine (A). Compared with the CdS-*Chi*-modified and bare electrodes, the CdS-*Chi*/*Gel*-modified electrode exhibited the highest electrocatalytic activity. The contact angle, a measure of the surface wettability, was used to determine the hydrophilicity of the CdS-*Chi* surface. SEM and AFM studies revealed morphological differences among the CdS-*Chi*-, *Gel*- and CdS-*Chi*/*Gel*-modified electrodes. Differential pulse voltammetry (DPV) measurements provided qualitative and quantitative characterization of the CdS-*Chi*/*Gel* electrode, even at physiologically relevant conditions. Therefore, this work establishes and demonstrates a simple and novel approach for the development of a biosensor based on transparent electrodes or ITO electrodes. This feature enables clinical applications for this real time biosensor.

Acknowledgments

The authors extend their appreciation to the Deanship of Scientific Research at King Saud University for funding the work through the research group project No. RGP-VPP-195.

References

[1] A.R. Lehmann, DNA Repair 10 (2011) 730.
[2] Y. Nakazawa, S. Yamashita, A.R. Lehmann, T. Ogi, DNA Repair 9 (2010) 506.
[3] L. Staresincic, A.F. Fagbemi, J.H. Enzlin, A.M. Gourdin, N. Wijgers, I.D. Sauthier, G.G. Mari, S.G. Clarkson, W. Vermeulen, O.D. Scharer, EMBO J. 28 (2009) 1111.
[4] D.A. Reeves, H. Mu, K. Kropachev, Y. Cai, S. Ding, A. Kolbanovskiy, M. Kolbanovskiy, Y. Chen, J. Krzeminski, S. Amin, D.J. Patel, S. Broyde, N.E. Geacintov, Nucl. Acids Res. 39 (2011) 8752.
[5] T. Furukawa, M.J. Curtis, C.M. Tominey, Y.H. Duong, B.W.L. Wilcox, D. Aggoune, J.B. Hays, A.B. Britt, DNA Repair 9 (2010) 940.
[6] J.B. Hays, DNA Repair 10 (2011) 526.
[7] F. Feng, H. Wang, L. Han, S. Wang, J. Am. Chem. Soc. 130 (2008) 11338.
[8] S. Pan, J. Xu, Y. Shu, F. Wang, W. Xia, Q. Ding, T. Xu, C. Zhao, M. Zhang, P. Huang, S. Lu, Biosens. Bioelectron. 26 (2010) 850.
[9] J.D. Suter, D.J. Howard, H. Shi, C.W. Caldwell, X. Fan, Biosens. Bioelectron. 26 (2010) 1016.
[10] T. Liu, J. Zhao, D. Zhang, G. Li, Anal. Chem. 82 (2010) 229.
[11] A.H. Badran, J.L. Furman, A.S. Ma, T.J. Comi, J.R. Porter, I. Ghosh, Anal. Chem. 83 (2011) 7151.
[12] R. Kurita, K. Arai, K. Nakamoto, D. Kato, O. Niwa, Anal. Chem. 84 (2012) 1799.
[13] Y. Li, C. Huang, J. Zheng, H. Qi, Biosens. Bioelectron. 38 (2012) 407.
[14] J. Hu, C.Y. Zhang, Biosens. Bioelectron. 31 (2012) 451.
[15] H. Matusiewicz, M. Ślachciński, Microchem. J. 102 (2012) 61.
[16] M. Su, W. Wei, S. Liu, Anal. Chim. Acta 704 (2011) 16.
[17] M.H. Ghanim, M.Z. Abdullah, Talanta 85 (2011) 28.
[18] H.J. Zeng, R. Yang, Q.W. Wang, J.J. Li, L.B. Qu, Food Chem. 127 (2011) 842.
[19] H.M. Qiu, Y.L. Xi, F.G. Lu, L.L. Fan, Spectrochim. Acta A 86 (2012) 456.
[20] H. Yu, Y.F. Tao, D.M. Chen, Y.L. Wang, L.G. Huang, D.P. Peng, M.H. Dai, Z.L. Liu, X. Wang, Z.G. Yuan, J. Chromatogr. B 879 (2011) 2653.
[21] H. Yu, Y.F. Tao, D.M. Chen, Y.H. Pan, Z.L. Liu, Y.L. Wang, L.G. Huang, M.H. Dai, D.P. Peng, X. Wang, Z.G. Yuan, J. Chromatogr. B 885/886 (2012) 150.
[22] T. Kamei, Proc. Eng. 25 (2011) 709.
[23] H.C. Chen, Y.S. Chang, S.J. Chen, P.L. Chang, J. Chromatogr. A 1230 (2012) 123.
[24] A. Santalad, L. Zhou, F.J. Shang, D. Fitzpatrick, R. Burakham, S. Srijaranai, J.D. Glennona, J.H.T. Luong, J. Chromatogr. A 1217 (2010) 5288.
[25] X.W. Zhang, Z.X. Zhang, J. Pharm. Biomed. Anal. 56 (2011) 330.
[26] S.M. Chen, C.H. Wang, K.C. Lin, Int. J. Electrochem. Sci. 7 (2012) 405.
[27] C. Tang, U. Yogeswaran, S.M. Chen, Anal. Chim. Acta 636 (2009) 19.
[28] D. Kato, N. Sekioka, A. Ueda, R. Kurita, S. Hirono, K. Suzuki, O. Niwa, J. Am. Chem. Soc. 130 (2008) 3716.
[29] D. Kato, N. Sekioka, A. Ueda, R. Kurita, S. Hirono, K. Suzuki, O. Niwa, Angew. Chem. Int. Ed. 47 (2008) 6681.
[30] X.X. He, J. Su, Y.H. Wang, K.M. Wang, X.Q. Ni, Z.F. Chen, Biosens. Bioelectron. 28 (2011) 298.
[31] K. Tanaka, K. Tainaka, T. Kamei, A. Okamoto, J. Am. Chem. Soc. 129 (2007) 5612.
[32] K. Tanaka, K. Tainaka, T. Umemoto, A. Nomura, A. Okamoto, J. Am. Chem. Soc. 129 (2007) 14511.
[33] Y.K. Ye, H.X. Ju, Biosens. Bioelectron. 21 (2005) 735.
[34] Q. Shen, X. Wang, J. Electroanal. Chem. 632 (2009) 149.
[35] Z.H. Zhu, X. Li, Y. Zeng, W. Sun, Biosens. Bioelectron. 25 (2010) 2313.
[36] A. Feráncova, S. Rengaraj, Y. Kim, J. Labuda, M. Sillanpää, Biosens. Bioelectron. 26 (2010) 314.
[37] H. Shiraishi, T. Itoh, H. Hayashi, K. Takagi, M. Sakane, T. Mori, J. Wang, Bioelectrochemistry 70 (2007) 481.
[38] P. Singhal, W.G. Kuhr, Anal. Chem. 69 (1997) 4828.
[39] Z.H. Wang, S.F. Xiao, Y. Chen, J. Electroanal. Chem. 589 (2006) 237.
[40] A.M.O. Brett, J.A.P. Piedade, L.A. Silva, V.C. Diculescu, Anal. Biochem. 332 (2004) 321.
[41] F. Boussicault, M. Robert, Chem. Rev. 108 (2008) 2622.
[42] T.A. Ivandini, K. Hond, T.N. Rao, A. Fujishim, Y. Einag, Talanta 71 (2007) 648.
[43] M. Zhou, Y. Zhai, S. Dong, Anal. Chem. 81 (2009) 5603.
[44] P. Sahoo, S. Dhara, S. Dash, A.K. Tyagi, Nanosci. Nanotechnol. Asia 1 (2011) 140.
[45] F. Patolsky, C.M. Lieber, Mater. Today 8 (2005) 20.
[46] Y. Umasankar, B. Unnikrishnan, S.M. Chen, T.W. Ting, Int. J. Electrochem. Sci. 7 (2012) 484.
[47] Y. Li, S.Y. Yang, C. Shen-Ming, Int. J. Electrochem. Sci. 6 (2011) 3982.
[48] J.Y. Yang, Y. Li, S.M. Chen, K.C. Lin, Int. J. Electrochem. Sci. 6 (2011) 2223.
[49] Y. Li, C.Y. Yang, S.M. Chen, Int. J. Electrochem. Sci. 6 (2011) 4829.
[50] M. Rajkumar, S.C. Chiou, S.M. Chen, S. Thiagarajan, Int. J. Electrochem. Sci. 6 (2011) 3789.
[51] Y. Li, J.X. Wei, S.M. Chen, Int. J. Electrochem. Sci. 6 (2011) 3385.
[52] Y. Li, S.M. Chen, W.C. Chen, Y.S. Li, M.A. Ali, F.M.A. AlHemaid, Int. J. Electrochem. Sci. 6 (2011) 6398.
[53] I. Willner, R. Baron, B. Willner, Biosens. Bioelectron. 22 (2007) 1841.
[54] M.M. Ardakani, Z. Taleat, H. Beitollahi, M.S. Niasari, B.B.F. Mirjalili, N. Taghavinia, J. Electroanal. Chem. 624 (2008) 73.
[55] H. Liu, G. Wang, D. Chen, W. Zhang, C. Li, B. Fang, Sens. Actuators B 128 (2008) 414.
[56] L.L. Zhang, J.J. Zhao, H. Zhang, J.H. Jiang, R.Q. Yu, Biosens. Bioelectron. 44 (2013) 6.
[57] P. Sorlier, A. Denuziere, C. Viton, A. Domard, Biomacromology 2 (2001) 765.
[58] A. Lahiji, A. Sohrabi, D.S. Hungerford, C.G. Frondoza, J. Biomed. Mater. Res. 51 (2000) 586.
[59] X. He, R. Yuan, Y. Chai, Y. Shi, J. Biochem. Biophys. Methods 70 (2007) 823.
[60] P. Wang, H. Wu, Z. Dai, X.Y. Zou, Biosens. Bioelectron. 26 (2011) 3339.